A&A manuscript no.
(will be inserted by hand later)

Your thesaurus codes are:
04.03.1, 04.19.1, 10.19.3, 13.09.6

ASTRONOMY
AND
ASTROPHYSICS
24.9.1996

First results from the ISOCAM parallel mode*

R. Siebenmorgen[1], A. Abergel[2], B. Altieri[1], A. Biviano[1,3], J.A.D.L. Blommaert[1], O. Boulade[4], C. Cesarsky[4], P. Gallais[4,1], S. Guest[5,1], M.F. Kessler[1], L. Metcalfe[1], K. Okumura[1], S. Ott[1], M. Perault[2], A.M.T. Pollock[1], T. Prusti[1], A. Sauvageon[4], J.L. Starck[4]

[1] ISO Science Operations Centre, Astrophysics Division of ESA, Villafranca del Castillo, P.O. Box 50727, E-28080 Madrid
[2] IAS, CNRS, Bat 121, University of Paris Sud, F-91405 Orsay
[3] Istituto T.E.S.R.E., CNR, via Gobetti 101, I-40129 Bologna
[4] CEA, DSM/DAPNIA, CE-Saclay, F-91191 Gif-sur-Yvette Cedex
[5] Rutherford Appleton Laboratory, Chilton, Didcot, Oxon OX11 0QX, England

Received ; accepted

Abstract. We present first results of a survey being made in a broad-band 6.75 μm filter using the ISOCAM infrared camera in its parallel mode at $\sim$ 6" resolution. So far we have analysed a sky area of ~ 1.375 deg^2 down to a limiting flux of 5 mJy and detected a total of 287 objects. The final survey will cover a sky area of $\sim$ 33 deg^2, most of which will be done in staring mode, to which we have restricted ourselves in the present paper. The final catalogue should reach a typical sensitivity limit of $\sim$ 1 mJy. We estimate that at the detection limit 99% of the objects will have a galactic origin.

Key words: Surveys – Galaxy: Structure – Infrared: stars

1. Introduction

The Infrared Space Observatory (ISO; Kessler et al., 1996) was successfully launched on 17th November 1995 with a complement of four instruments aboard including the infrared camera ISOCAM (Cesarsky et al., 1996). The first 78 orbits, each lasting roughly 23h54m, were designated the performance verification phase (PV), during which the mission check-out and prime calibration of the instruments and the telescope were performed.

In its so-called parallel mode, ISOCAM is routinely exposed in a broad filter centered at 6.75 μm to the sky between about 10' and 20' away from the prime target under observation by one of the three other instruments, thus enabling an effectively unbiased survey of limited areas of the infrared (IR) sky at high sensitivity. The field of view of ISOCAM is 3' $\times$ 3' and thus each field observed is roughly the equivalent of a single pixel of the IRAS survey, giving a fifteen-fold increase in angular resolution as some compensation for the far from complete solid-angle coverage anticipated. So far, we have analysed 19 orbits of ISOCAM parallel-mode data obtained during the PV, amounting to $\approx$ 300 hours of observing time.

2. Observations

During the performance verification phase ISOCAM was observing in the parallel mode in a fixed optical configuration. In this configuration the full field of view of the camera (3'$\times$ 3') is used. The pixel field of view (pfov) is set to 6". The amplifier gain g equals two. Every 2.1 sec the detector is read out. In the parallel mode the full telemetry rate is not available because one of the other ISO instruments is prime. Consequently not all individual exposures can be down-linked to the ground segment. As a result, twelve individual exposures have to be co-added on board, so that the quantum of a single ISOCAM parallel mode frame is 25.2 sec.

3. Data processing

The data processing for ISOCAM parallel mode data is similar to when ISOCAM is the prime instrument. The data reduction consists of (for details see Siebenmorgen et al., 1996):

- cosmic ray impact and glitch suppression.
- Normalizing the data to gain–adjusted analog digital units (ADU/s).
- The dark current subtraction.
- Flat field correction.

Send offprint requests to: rsiebenm@iso.vilspa.esa.es

* ISO is an ESA project with instruments founded by ESA Member States (especially the PI countries: France, Germany, the Netherlands and the United Kingdom) and with the participation of ISAS and NASA.

– Finally, averaging the stabilized pixel values corresponding to the same sky position. Taking the rms of the same pixels provides the statistical noise image.

The corresponding dark pattern, optical and detector flat fields are extracted from the calibration libraries.

3.1. Problems of reliable source detection

Parallel mode sometimes yields a small number of independent frames of data for a given pointing. This, along with the normal problems affecting all ISOCAM staring-mode data, leads to the following complications in the case of automatic processing:
i) The dark current shows statistical variations of about 0.3 ADU/s and long-term drifts of order 2 ADU/s.
ii) At present the residual non-uniformities after flat-fielding of staring-mode observations amount to about 2% for the central pixels and up to 20% for pixels at the border of the detector array. This is due to lens wheel position jitter which causes the 6" pfov vignetting profile to move slightly over the detector. For a single pixel we typically observe a background level of order 5 ADU/s (~2.5 mJy) and this varies by about a factor of three depending on ecliptic latitude. This will introduce a typical numerical flat-field-based uncertainty of about ≤ 1 ADU/s. This implies that extended source detection becomes a non-trivial problem, because we can never exclude the possibility that we are detecting residual flat-field structure at a low level.
iii) As the pfov is matched to the point spread function (PSF) at $6.75\mu m$, each badly corrected glitch can lead to a false detection. Deglitching is not a trivial task for several reasons. In general the data are rarely stabilized and it takes a long time before the pixels reach their final values. Secondly, several glitches can successively hit the same pixel and create a long temporal structure. We must ensure that our detected sources are not artifacts such as remnants of glitches. For these reasons, we use a Multi-resolution Median Transform algorithm (MMT; Starck et al., 1995). The MMT method is well adapted to the deglitch problem if the number of frames $n \geq 10$. For observations where $5 \leq n < 10$ we use a conventional temporal deglitch method and do not consider observations with fewer than 5 individual frames. As a consequence no observations which integrate less than 5×25.2s on a single sky position can be deglitched and so are not considered here. One has further to take into account that there is no perfect deglitching algorithm available yet and each of the methods used here have their own pitfalls. The deglitching methods still do not remove all long term gain fluctuations, which are of the order of 1 ADU/s.
iv) Concerning the memory effect and flux transients, we have considered a pixel signal as stabilized, if it is within 10% of its final value. In our automatic processing we have not used any model for flux transient corrections, nor field of view distortion or special treatments for raster images. Neither have we analysed any data obtained from parallel mode while the satellite was slewing.

3.2. Threshold for source detection

Automatic reduction algorithms leave a number of anomalies in the data. Several of these (e.g. dark current drift or residual glitches) are independent of background flux, and so we have set a fixed numerical threshold for a source detection. Adding the effects of the above uncertainties (Sect. 3.1) results in a threshold of 10 ADU/s for source detection at 5σ level. A side benefit of having such a fixed threshold is that the sensitivity limit is a fixed flux-density of 5mJy, rather than being a variable, background-dependent limit.
The theoretical sensitivity limit for staring observations is approached asymptotically for dwell times greater than about 150 seconds (or about 6 parallel mode frames). After this time one will have detected sources down to about 2 ADU/s (1 mJy) at 10 σ. Further dwell time will not improve the sensitivity. This theoretical limit is proportional to the local background flux. Eventually, when these various sources of uncertainty in the data can be reliably corrected and the detection limit becomes flat-field driven then the meaningful threshold for source detection will best be defined in terms of proportionality to the background.

3.3. Method of source detection

Since the PSF in the 6" lens is well-covered by a small number of pixels (≈ 3), we can simply apply a median filter for the background estimate. For this we use a box with a size of 7×7 pixels on each image, which removes all the point sources. Events where the signal is ≥ 10 ADU/s above the background are considered as reliable detections at $\geq 5\sigma$.
For each pixel of the final calibrated image, we indicate by means of a boolean detection image, whether or not it fulfils the detection criteria. The boolean detection image allows an indication as to whether a source may show the signature of extended emission. We speak of extended emission if detections are clustered together in a box of more than 3×3 pixels. Even if all pixels in a box of $\leq 3 \times 3$ fulfil the detection criteria, the source is still considered point-like.
The source photometry is performed on all pixels associated with a source. We find that a large part of the uncertainty of the photometry is introduced by the background estimate. For extended sources with large structures it is possible that the method will split up a single source into several structures, which would all be counted as individual sources. For this reason we have introduced a confusion flag in our final source list. For each source we calculate the number of associations with other sources in our list. This is done by taking a radius around the

source center equal to the source size as calculated from the linear extension of the clustered pixels in the boolean detection map. For point sources we use a radius of 3 pixels. If we find any other source(s) within this radius we consider the source to be confused. As the centre of a source we simply take the brightest pixel, for which we give the celestial position. We have compared this simple approach with other estimates of source positions using fitting methods and the PSF, and we find the same coordinates to within a fraction of a pixel (this is owing to the fact that the 6" PSF is well-covered within $\approx$ 3 pixels). Consequently, for each source, its extension in pixels, integrated flux, statistical noise, celestial coordinates and number of associations (confusion) are known.

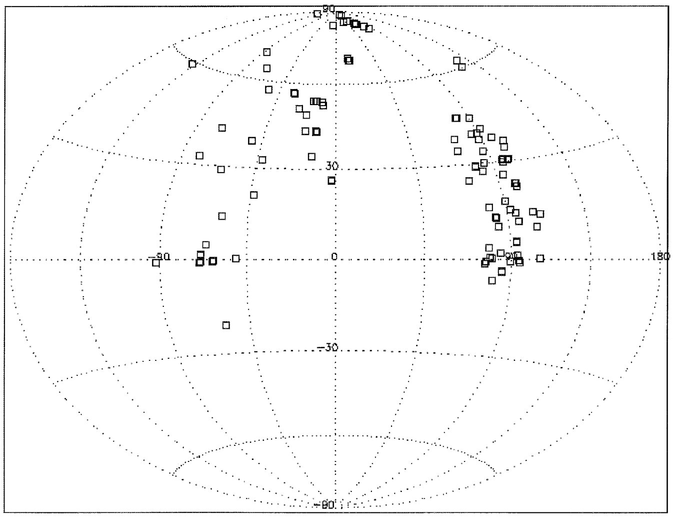

Fig. 1. Pointings of the ISO satellite are shown (squares) in galactic coordinates for all revolutions analysed in this article.

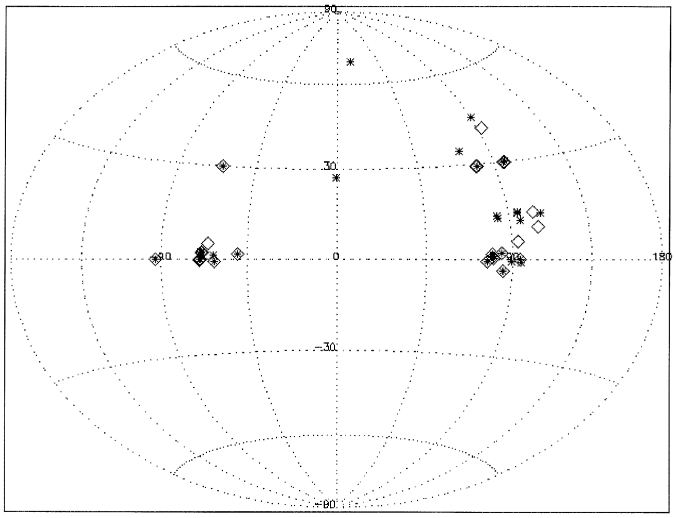

Fig. 2. Distribution of sources in galactic coordinates. Point-like sources are represented by stars and extended sources by diamonds.

4. Results

We have analysed 6 PV phase calibration revolutions of the long wavelength spectrometer ISOLWS (Clegg et al., 1996) and 13 calibration revolutions of the photometer ISOPHOT (Lemke et al., 1996). Roughly speaking we find one detection for every single hour of observing in the ISOCAM parallel mode. Taking this detection rate and assuming a 24 month lifetime of ISO, the final catalogue size will be in excess of 10^4 individual sources. Querying the present ISO proposal database gives a number of about 15000 individual telescope pointings with ISOCAM in parallel mode. Considering the field of view of ISOCAM there will be about 33 deg^2 of the sky covered by this survey. About 90% of those pointings will be performed in such a way that ISOCAM will observe a single sky position. For the remaining parallel mode observations the prime instrument will move by a small step size, so that one can expect to have micro-scan images. The fundamental sensitivity limit will be about 1 mJy for the staring observations and, thanks to the improved flat-field, about 0.1 mJy for the micro scans. However, the rasters will cover only a small total solid angle on the sky.

5. Discussion

Some simple statistical arguments may give clues as to the nature of the population of sources. For the PV phase, the ISO satellite pointings shown in Figure 1 and the detected sources in Figure 2 show that most attention has, not surprisingly, been confined to the galactic disk; although 19 sources have been detected at high galactic latitudes. Half of the objects with $\mid b \mid > 30°$ have an optical counterpart on the Digital Sky Survey (DSS), but are neither listed in the IRAS Faint Source Catalogue nor in any catalogue of galactic or extragalactic objects. By searching with SIMBAD, one object could be unambiguously identified as the catalogue source [HH87]61 (Hacking & Houck, 1987) at a 6.75 μm flux of 25 ± 5 mJy. The other half of the sources at $\mid b \mid > 30°$ had no clear optical counterpart on the DSS, with several faint sources around the position in the DSS or a blank field.

The cumulative number of sources, $\log(N > F_{6.75\mu m})$, as a function of source flux, $\log(F_{6.75\mu m})$, for low galactic latitude $\mid b \mid < 2.5°$ is shown in Figure 3. Our complete sample and additionally a sub–sample of point sources are shown. It can be seen that sources have a typical flux at 6.75 μm of between 5 to 300 mJy. The point sources are detected with fluxes between 5 and 70 mJy. Following Wainscoat et al. (1992), we expect to see that most of the stars are from the exponential disk component, except for: i) The regions of low galactic latitude, where there are contributions from the spiral arms, ii) the molecular ring and iii) near the Galactic center (GC) where the bulge becomes important. One of the main scientific results we hope to obtain after completion of this survey is a detailed decomposition of these individual populations. Our present detection limit of 5 mJy corresponds, assuming a black body stellar spectrum, to an equivalent of about $m_K \approx 10$ mag. This number already suggests that cross-correlation with near infrared catalogues, such as the future DENIS database (Forveille et al., 1992), should make it possible to derive a large amount of colour information of late type stars. Such information is of particular importance to improve our knowledge of processes such as the mass loss phenomena of AGB stars and/or super-giants. In order to derive a better understanding of the characteristics of objects nearby the GC one needs: i) high angular resolution, in order to reduce the source confusion, and ii) observation in the near and mid IR, owing to the high extinction towards the GC. Similar observational requirements are also given for systematic searches of protostellar candidates in dense regions. In both cases, ISOCAM parallel mode observations have a high potential to improve the present knowledge.

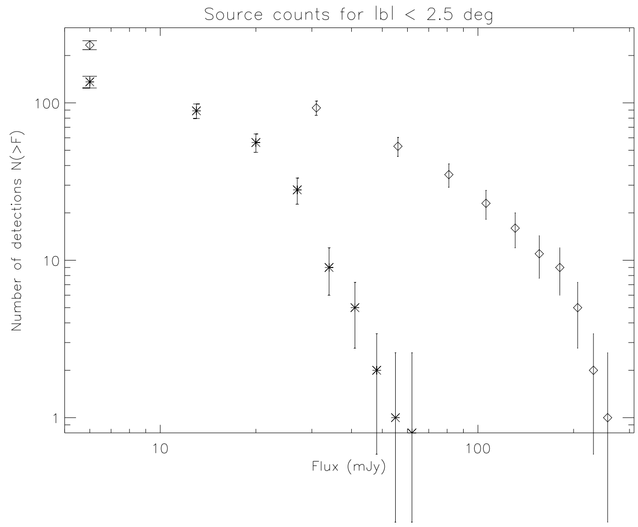

Fig. 3. Cumulative number of sources as a function of source flux, $\log(N > F_{6.75\mu m})$ vs. $\log(F_{6.75\mu m})$, for $\mid b \mid < 2.5°$. The full sample (diamonds) and a sub–sample of point like sources (stars) are shown.

This survey will contribute to testing evolutionary models of galaxy formation. Cesarsky et al. (1993) give the integral source counts of galaxies expected at 6.7 μm, assuming the cosmological parameters $H_0 = 50$ km/s/Mpc, and $q_0 = 0.5$, and a time of galaxy formation of 2 Gyr for spirals and 1 Gyr for E/S0. They predict a number density of galaxies brighter than 5 mJy of 2×10^{-4} arcmin^{-2}. In our present sample, we have 550 independent pointings, corresponding to a surveyed area of 4950 arcmin^2, so we expect to detect about one galaxy. The fact that we have not yet identified a single galaxy is therefore consistent with this estimate. With the data-reduction technique described in this paper, and considering only staring observations, we expect to have detected $\simeq 30$ galaxies by the end of the ISO mission, most of which are expected to be normal spirals. This number will be increased by applying the 1 mJy detection limit and even more by including deep raster observations where the limiting flux is about 0.1 mJy. At this flux limit, the number density of galaxies (at 6.7 μm) rises to 9×10^{-3} arcmin^{-2}. Given the expected number of deep raster observations over the whole ISO mission ($\sim$ 1500) we expect to detect $\sim$ 120 galaxies, about half of which would be Seyfert galaxies. The achievable limit in redshift z, depends on the intrinsic brightness of the objects. A bright Seyfert galaxy like Mrk 231 could be detected as far as z=0.5 with the present strategy, and to as far as z=1.5 with the deep raster observations. If a bright quasar (like 3C273) is considered, then the present strategy would detect it as far as z=1.0, and when deep raster observations are considered, it would be detected as far as z=4.0. However, given the rarity of such objects (one per 10000 Seyferts, Woltjer 1990) we do not expect any of these objects from this survey.

References

Cesarsky C., et al., 1996, A&A this issue
Cesarsky C., Chase S.T., Danese L., Desert F.-X., Franceschini, in: "ISOCAM Guaranteed Time Proposal" (ISO preprint)
Clegg P.E., et al., 1996, A&A this issue
Hacking P., and Houck J.R., 1987, ApJSS 63, 311
Kessler M.F., et al., 1996, A&A this issue
Lemke D., et al., 1996, A&A this issue
Forveille T., Epchstein N., Burton W.B., 1992, in: "Infrared Astronomy with ISO", Les Houches, Th. Encrenaz and M.F. Kessler (eds.), Nova Science Publ. Co., p. 525.
Siebenmorgen R., Starck J.L., Cesarsky D.A., Guest S., Sauvage M., 1996, "ISOCAM Data Users Manual Version 2.1", ESA document, Reference: SAI/95-222/Dc.
Starck J.L., Bijaoui A., Murtagh F., 1995, in: "Multiresolution Support Applied to Image Filtering and Deconvolution", in CVIP: Graphical Models and Image Processing, Vol. 57, 5, p. 420.
Wainscoat R.J., Cohen M., Volk K., Walker H.J., Schwarz D.E., 1992, ApJSS 83, 111.
Woltjer L. 1990, in: "Active Galactic Nuclei", proceedings of the Saas-Fee Advanced Course n.20, eds.: Courvoisier, T.J.-L., and Mayor, M., Springer-Verlag, Berlin.

This article was processed by the author using Springer-Verlag LaTeX A&A style file *L-AA* version 3.